

A 750 GeV dark matter messenger at the Galactic Center

Xian-Jun Huang, Wei-Hong Zhang, Yu-Feng Zhou

Key Laboratory of Theoretical Physics,

Institute of Theoretical Physics, Chinese Academy of Sciences

Beijing, 100190, P.R. China

(Dated: May 24, 2016)

The first data from the LHC Run-2 have shown a possible excess in diphoton events with invariant mass ~ 750 GeV, suggesting the existence of a new resonance which may decay dominantly into dark matter (DM) particles. We show in a simple model that the reported diphoton excess at the LHC is consistent with another photon excess, the 2 GeV excess in cosmic gamma-ray fluxes towards the Galactic Center observed by the Fermi-LAT. Both the excesses can be simultaneously explained by a ~ 60 GeV scalar DM particle annihilating dominantly into two gluons with a typical thermal annihilation cross section, which leads to the prediction of a width to mass ratio $\Gamma/M \approx \mathcal{O}(10^{-2})$ of the resonance. The upper limit on the dijet search at LHC Run-1 leads to a *lower* limit on the predicted cross section for DM annihilating into $\gamma\gamma$ final states $\langle\sigma v\rangle_{\gamma\gamma} \gtrsim \mathcal{O}(10^{-30}) \text{ cm}^3\text{s}^{-1}$. Both the predictions can be tested by the LHC, Fermi-LAT and future experiments.

Introduction. Recently, the ATLAS and CMS collaborations have reported the first data from the LHC Run-2 at $\sqrt{s} = 13$ TeV, based on the integrated luminosity of 3.2 fb^{-1} and 2.6 fb^{-1} , respectively [1]. Both the collaborations have shown a possible excess in diphoton events, suggesting the existence of a new resonance particle ϕ with mass $M \approx 750$ GeV. The distribution of the observed events at ATLAS favours a width to mass ratio of the resonance $\Gamma/M \approx 0.06$ with a local (global) significance of 3.9σ (2.6σ). The CMS collaboration has reported a mild peak at ~ 760 GeV with a local (global) significance of 2.6σ (1.2σ) and slightly favours a narrow width. Assuming a large width, the ATLAS (CMS) data favour a production cross section $10 \pm 3 \text{ fb}$ ($6 \pm 3 \text{ fb}$) [2]. Other analyses assuming narrow width give ~ 6.2 (5.6) fb for ATLAS (CMS) [3]. Recent updates from both ATLAS and CMS have shown that a mild upward fluctuation at 750 GeV also exists in the Run-1 data at 8 TeV. The local (global) significance of the diphoton excess in the combined CMS data of 8+13 TeV has increased to 3.4σ (1.6σ) [4].

The excess, if not due to statistic fluctuations, can be an intriguing clue of new physics beyond the standard model (SM): the resonance ϕ should not be the only new particle. If the observed number of diphoton events are explained by the usual

loop processes involving *only* the SM particles, ϕ should decay into these SM particles appearing in the loop with large rates, which is inconsistent with the LHC Run-1 data [5, 6]. Furthermore, ϕ should have extra tree-level invisible decays if the large width reported by ATLAS is confirmed. An interesting possibility is that the dark matter (DM) particle is among the decay final states of ϕ [2, 7–16]. In this scenario, ϕ plays a role of messenger connecting the invisible and visible sectors by making the DM particles couple to gluons and photons through ϕ -exchange, which has rich phenomenological consequences.

Note that there is another photon related excess. Recently, a number of groups have independently found statistically strong evidence of an excess in cosmic gamma-ray fluxes at ~ 2 GeV towards the inner regions around the Galactic center (GC) from the data of Fermi-LAT [17–30]. The morphology of this GC excess (GCE) emission is consistent with a spherical emission profile expected from DM annihilation [22, 23, 26, 29]. The determined energy spectrum of the excess emission is in general compatible with a DM particle self annihilating into $b\bar{b}$ final states with a typical thermal annihilation cross section [26, 28]. Plausible astrophysical explanations also exist, such as the unresolved point sources of mili-second pulsars [20–23, 31, 32] and

the interactions between the cosmic rays and the molecular gas [24, 25, 33].

In this work, we show that the two reported photon excesses can be closely connected. They can be simultaneously explained by a simple scalar DM model with a light DM particle mass ~ 60 GeV and a typical thermal annihilation cross section, which leads to the predictions that *i*) the resonance should have a large width, $\Gamma/M \gtrsim \mathcal{O}(10^{-2})$ from the required DM mass and annihilation cross section; *ii*) the upper limit on the dijet search at LHC Run-1 leads to a *lower* limit on the predicted cross section $\langle\sigma v\rangle_{\gamma\gamma} \gtrsim \mathcal{O}(10^{-30}) \text{ cm}^3\text{s}^{-1}$ for DM annihilating into $\gamma\gamma$ with a line-shape gamma-ray spectrum. Both of them can be tested by the LHC, Fermi-LAT and future experiments.

Effective interactions. We consider a simple model where the resonance ϕ is a pseudo-scalar particle and the DM particle χ with mass m_χ is a real scalar. The interactions related to ϕ and χ is given by

$$\mathcal{L}_{\phi\chi} \supset \frac{1}{2}(\partial_\mu\phi)^2 + \frac{1}{2}(\partial_\mu\chi)^2 - \frac{1}{2}M^2\phi^2 - \frac{1}{2}m_\chi^2\chi^2 - \frac{1}{2}g_\chi\phi\chi^2, \quad (1)$$

where g_χ is the dimensionful $\phi\chi\chi$ coupling strength. The resonance ϕ can couple to the SM gauge fields typically through loop processes (see e.g. Refs. [34]). Since ϕ is much heavier than the electroweak (EW) scale, we start with effective dimension-five EW gauge-invariant interactions

$$\mathcal{L} \supset \frac{g_1^2}{2\Lambda}\phi B_{\mu\nu}\tilde{B}^{\mu\nu} + \frac{g_2^2}{2\Lambda}\phi W_{\mu\nu}\tilde{W}^{\mu\nu} + \frac{g_g^2}{2\Lambda}\phi G_{\mu\nu}\tilde{G}^{\mu\nu}, \quad (2)$$

where for the gauge fields $\tilde{F}_{\mu\nu} = \frac{1}{2}\epsilon_{\mu\nu\alpha\beta}F^{\alpha\beta}$, $g_{1,2,g}$ are the dimensionless effective coupling strengths, and Λ is a common energy scale. After the EW symmetry breaking, the interaction terms involving physical EW gauge bosons A , Z and W^\pm are

$$\mathcal{L} \supset \frac{g_A^2}{2\Lambda}\phi A_{\mu\nu}\tilde{A}^{\mu\nu} + \frac{g_Z^2}{2\Lambda}\phi Z_{\mu\nu}\tilde{Z}^{\mu\nu} + \frac{g_{AZ}^2}{2\Lambda}\phi A_{\mu\nu}\tilde{Z}^{\mu\nu} + \frac{g_W^2}{2\Lambda}\phi W_{\mu\nu}\tilde{W}^{\mu\nu} + \frac{g_g^2}{2\Lambda}\phi G_{\mu\nu}\tilde{G}^{\mu\nu}, \quad (3)$$

where the couplings $g_{A,Z,ZA,W}$ are related to the couplings in Eq. (2) as $g_A^2 = g_1^2 c_W^2 + g_2^2 s_W^2$, $g_Z^2 =$

$g_1^2 s_W^2 + g_2^2 c_W^2$, $g_{ZA}^2 = 2s_W c_W (g_2^2 - g_1^2)$, and $g_W^2 = g_2^2$ with $s_W^2 = 1 - c_W^2 = \sin^2\theta_W \approx 0.23$. The partial decay widths for the decays $\phi \rightarrow \gamma\gamma$, gg and $\chi\chi$ are given by

$$\frac{\Gamma_{\gamma\gamma}}{M} = \pi\alpha_A^2 \left(\frac{M}{\Lambda}\right)^2, \quad \frac{\Gamma_{gg}}{M} = 8\pi\alpha_g^2 \left(\frac{M}{\Lambda}\right)^2, \quad \frac{\Gamma_{\chi\chi}}{M} = \frac{g_\chi^2\beta_\chi}{32\pi M^2}, \quad (4)$$

respectively, where $\alpha_{A,g} = g_{A,g}^2/4\pi$, and $\beta_\chi = (1 - 4m_\chi^2/M^2)^{1/2}$ is the velocity of the final state DM particles in the ϕ rest frame.

The UV origins of the pseudoscalar ϕ can be axion-like particles from the breaking of the Peccei-Quinn symmetry [35], pseudo-Goldstone boson from composite Higgs models [36], or from the extended Higgs sectors such as the two-Higgs-doublet models. If ϕ is a SM singlet and couples to the SM gauge bosons through new vector-like heavy fermions which have small mixings with the SM fermions, the constraints from the oblique parameters S and T , the EW precision test, and the flavor physics can be evaded [37]. Since ϕ is a pseudo-scalar, it does not mix directly with the SM Higgs boson. Thus is less constrained by the measured properties of the SM Higgs boson. Furthermore, the DM-nucleus scattering matrix element for gluons $\langle N | G_{\mu\nu}^a \tilde{G}^{a\mu\nu} | N \rangle$ is vanishing as the operator $G_{\mu\nu}^a \tilde{G}^{a\mu\nu}$ is CP-odd, which makes the DM particles easily evade the stringent constraints from DM direct detection experiments.

Diphoton excess. We shall focus on the case where the reported $\gamma\gamma$ excess at the LHC is generated by gluon-fusion through the s -channel ϕ -exchange. Other non-resonant mechanisms have also been considered (see e.g. in Refs. [38]). In the narrow width approximation, the production cross section for diphoton (dijet) is given by

$$\sigma_{\gamma\gamma(jj)} \approx \frac{C_{gg}}{s(\Gamma/M)} \left(\frac{\Gamma_{gg}}{M}\right) \left(\frac{\Gamma_{\gamma\gamma(gg)}}{M}\right), \quad (5)$$

where the coefficient C_{gg} incorporates the convolution over the gluon parton distribution functions of the proton. At $\sqrt{s} = 13$ (8) TeV, $C_{gg} \approx 2137$ (174) [2]. Higher order QCD corrections can be taken into account by the K -factors with typically $K_{gg} \approx$

1.48. Making use of Eq. (4), the products of the couplings required to reproduce the diphoton excess can be estimated as

$$\left(\frac{\alpha_A}{0.01}\right)^2 \left(\frac{\alpha_g}{0.1}\right)^2 \left(\frac{M/\Lambda}{0.18}\right)^4 \approx \left(\frac{\sigma_{\gamma\gamma}}{8 \text{ fb}}\right) \left(\frac{\Gamma/M}{0.06}\right). \quad (6)$$

Thus the common scale Λ can still be larger than the mass of the resonance ϕ , although not significantly larger. For weakly coupled models, large effective couplings can be obtained by introducing multiple heavy intermediate particles running in the loop. A large total width $\Gamma/M \sim 0.06$ can be obtained by additional ϕ decay channels, such as decay into DM particles. Including the invisible decay $\phi \rightarrow \chi\chi$, the total width is

$$\Gamma = \Gamma_{\chi\chi} + \Gamma_{gg} + \kappa\Gamma_{\gamma\gamma}, \quad (7)$$

where $\kappa = 1 + (g_Z^4 + g_{ZA}^4/2 + 2g_W^4)/g_A^4$. If the total width Γ is dominated by $\Gamma_{\chi\chi}$, a large $\Gamma/M \approx 0.06$ requires an effective coupling $g_\chi^2/(4\pi M^2) \approx 0.5$ which is large but still within the perturbative regime.

Constraints already arise from the LHC Run-1 data on the searches for general resonances. For instance, $\sigma_{ZZ} \lesssim 12 \text{ fb}$ [41], $\sigma_{Z\gamma} \lesssim 4.0 \text{ fb}$ [42], and $\sigma_{WW} \lesssim 40 \text{ fb}$ [43, 44]. For the LHC Run-2 with ϕ produced from gluon fusion, it is expected that these upper bounds will be relaxed roughly by a factor $r = 0.38C_{gg}(13 \text{ TeV})/C_{gg}(8 \text{ TeV}) \approx 4.7$. The coupling between ϕ and the gluons is directly constrained by the null results of the search for dijet from a generic resonance at the Run-1, $\sigma_{jj} \lesssim 2.5 \text{ pb}$ [39]. If Γ is dominated by gg final states, one obtains a stringent limit $\Gamma_{gg}/M \lesssim 1.6 \times 10^{-3}$. However, if Γ is dominated by $\Gamma_{\chi\chi}$, the constraint can be significantly weaker. For $\Gamma/M \approx 0.06$, we find $\Gamma_{gg}/M \lesssim 1.1 \times 10^{-2}$. In this work, we consider a representative case where ϕ couples dominantly to the $U(1)$ gauge field, i.e. $g_2 = 0$. In this case, the $ZZ(Z\gamma)$ channel is suppressed as $\sigma_{ZZ(Z\gamma)}/\sigma_{\gamma\gamma} = 0.09$ (0.6). Note that in the opposite case where $g_1 = 0$, the cross section $\sigma_{ZZ(Z\gamma)}$ is enhanced by a factor of 11 (6.7), which is already severely constrained by the Run-1 data.

GC excess. In this model, the velocity-averaged DM annihilation cross section multiplied by the DM relative velocity for two gluons (photons) final states is given by

$$\langle\sigma v\rangle_{gg(\gamma\gamma)} \approx \frac{256\pi m_\chi^2 \left(\frac{\Gamma_{\chi\chi}}{M}\right) \left(\frac{\Gamma_{gg(\gamma\gamma)}}{M}\right)}{[(M^2 - 4m_\chi^2)^2 + M^2\Gamma^2] \beta_\chi}, \quad (8)$$

where we have neglected the p -wave contributions. We shall perform a combined χ^2 -analysis to both the diphoton excess at the LHC and the GCE from the Fermi-LAT to see if they can be consistently explained by a common parameter set $\{\Gamma_{gg}/M, \Gamma_{\chi\chi}/M, m_\chi\}$, for fixed values of Γ/M . For the diphoton excess, we take a naively weighted average of ATLAS and CMS results $\sigma_{\gamma\gamma} = 8 \pm 2.1 \text{ fb}$. The upper limit from the dijet process is taken into account by constructing a χ^2 -term corresponding to the 95% upper limit at Run-1, assuming Gaussian distribution. The GCE data are taken from Ref. [29]. The gamma-ray fluxes are calculated and averaged over a square region of interest (ROI) $20^\circ \times 20^\circ$ in the sky with latitude $|b| < 2^\circ$ masked out. In the calculation, we adopt a contracted NFW profile with inner slop $\gamma = 1.26$, as suggested by the observed morphology of the gamma-ray emission [22, 23, 26, 29], and is normalized to the local DM density $\rho_0 = 0.4 \text{ GeV} \cdot \text{cm}^{-3}$. The halo DM annihilation into gg generates diffuse gamma rays with a broad energy spectrum due to hadronization. The injection spectrum for DM annihilating into two gluons are generated by Pythia 8.201 [45].

We first perform a fit to the data of GCE alone. The result shows that a cross section close to the typical thermal cross section is favoured $\langle\sigma v\rangle_{gg} = (1.96_{-0.24}^{+0.26}) \times 10^{-26} \text{ cm}^3\text{s}^{-1}$ with a relatively small DM particle mass $m_\chi = 62.0_{-6.3}^{+6.6} \text{ GeV}$. The goodness of fit $\chi^2/\text{d.o.f} = 24.6/22$ indicates a good agreement with the data for DM annihilation into two gluons. A consequence of the required DM mass and annihilation cross section is that the total width Γ of ϕ cannot be too small. From the definition of Γ , it follows that $\Gamma^2 \gtrsim 4\Gamma_{gg}\Gamma_{\chi\chi}$, and a lower bound on the total width can be derived

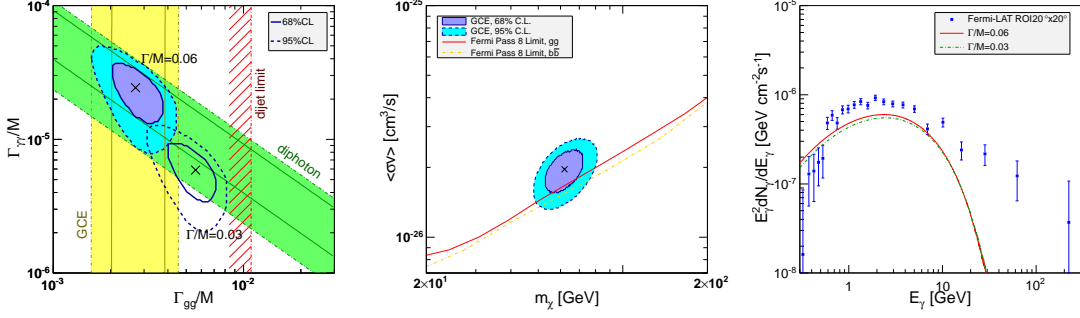


FIG. 1: Left) Allowed regions in $(\Gamma_{gg}/M, \Gamma_{\gamma\gamma}/M)$ plane at 68% C.L. (violet contour) and 95% C.L. (light-blue contour) from the combined fit to the data of diphoton excess [1], GCE [29] and the constraints from the Run-1 dijet search limits [39], for $\Gamma/M = 0.06$. The regions allowed by the individual experiment at 95% C.L. are also shown. The open contours correspond to a similar fit with $\Gamma/M = 0.03$. Middle) Allowed regions for the parameters $(m_\chi, \langle\sigma v\rangle_{gg})$ from the fit with $\Gamma/M = 0.06$, together with the conservative upper limits at 95% C.L. (solid curve) derived from the Fermi-LAT data on the gamma rays of dSphs for $b\bar{b}$ channel (dashed curve) [40]. See text for details. Right) Energy spectra of the gamma-ray fluxes from the best-fit parameters in Eq. (10) for $\Gamma/M = 0.06$ and 0.03, respectively, together with the GCE data derived in Ref. [29].

from Eq. (8)

$$\frac{\Gamma}{M} \gtrsim 0.023 \left(\frac{60 \text{ GeV}}{m_\chi} \right) \left(\frac{M}{750 \text{ GeV}} \right)^2 \frac{\langle\sigma v\rangle_{gg}^{1/2}}{\langle\sigma v\rangle_0^{1/2}}, \quad (9)$$

where $\langle\sigma v\rangle_0 = 1.5 \times 10^{-26} \text{ cm}^3\text{s}^{-1}$ is the cross section at the 2σ lower bound allowed by the GCE data. Thus a consistent explanation for the diphoton excess and the CGE predicts a minimal required value of $\Gamma/M \approx \mathcal{O}(10^{-2})$ which is favoured by the current ATLAS data, and can be tested by CMS and the future data.

In the combined fit, we consider two choices of total width, $\Gamma/M = 0.06$ favoured by the ATLAS data, and $\Gamma/M = 0.03$ which is close to the minimal allowed value by the GCE data. The results of the determined parameters are as follows

$$\begin{aligned} \Gamma_{gg}/M &= 2.7 \pm 0.4 \text{ } (5.6^{+0.9}_{-1.0}) \times 10^{-3}, \\ \Gamma_{\gamma\gamma}/M &= 2.4^{+0.8}_{-0.7} \text{ } (0.59^{+0.20}_{-0.17}) \times 10^{-5}, \\ m_\chi &= 63.7^{+6.6}_{-6.3} \text{ } (65.9^{+6.3}_{-4.9}) \text{ GeV}, \end{aligned} \quad (10)$$

with $\chi^2/\text{d.o.f} = 24.7/24$ ($26.9/24$) for $\Gamma = 0.06$ (0.03). The allowed regions in the $(\Gamma_{gg}/M, \Gamma_{\gamma\gamma}/M)$ plane at 68% and 95% C.L. for two parameters, corresponding to $\Delta\chi^2 = 2.3$ and 6.0, respectively, are

shown in the left panel of Fig. 1, together with the allowed regions by each individual experiment. For $\Gamma/M = 0.06$, the total χ^2 is almost unchanged compared with that from the fit to the GCE data alone, which shows that the diphoton excess, GCE and dijet limits can be made consistent with each other within this model. While for $\Gamma/M = 0.03$, a slightly larger χ^2 is obtained, which is mainly due to the tension between the Run-1 dijet constraint and the total width as can be seen from Eq. (9).

In the middle panel of Fig. 1 we show the allowed regions for the parameters $(m_\chi, \langle\sigma v\rangle_{gg})$ at 68% and 95% C.L.. At present, the most stringent constraint on the DM annihilation cross sections are provided by the Fermi-LAT data on the diffuse gamma rays of the dwarf spheroidal satellite galaxies (dSphs) [40]. We make a conservative estimation of the limit on the cross section for the gg final states based on the known limit on that for the $b\bar{b}$ final states from the 6-year Fermi-LAT data as follows. For a gamma-ray spectrum $dN_\gamma^{(b\bar{b})}/dE$ generated from DM annihilation into $b\bar{b}$ with given values of m_χ and $\langle\sigma v\rangle_{b\bar{b}}$, we search for a cross section $\langle\sigma v\rangle_{gg}$ for the gg channel with a DM particle mass m'_χ which satisfies the condition that dN_γ^{gg}/dE is just above $dN_\gamma^{(b\bar{b})}/dE$ for all the gamma-ray en-

ergies. The Fermi-LAT limit on $\langle\sigma v\rangle_{b\bar{b}}$ at m_χ is then estimated as a conservative limit on $\langle\sigma v\rangle_{gg}$ at m'_χ . The resulting limits are shown in Fig. 1, together with that for the $b\bar{b}$ final states. As can be seen from the figure, the two limits are quit similar. There is a possible tension between the GCE favoured regions and the Fermi-LAT limits. Note that in the analysis of the Fermi-LAT collaboration, the uncertainties in the J -factors were taken into account assuming a NFW type parametrization of the DM density profile. A recent analysis directly using the spherical Jeans equations rather than taking a parametric DM density profile as input showed that the J -factor can be smaller by a factor about 2 – 4 for the case of Ursa Minor, which relaxes the constraints on the DM annihilation cross section to the same amount [46]. In the right panel of Fig. 1, we show the gamma-ray spectra for the best-fit parameters in Eq. (10), together with the Fermi-LAT data [29]. Although the predicted spectra look slightly lower than the data, the obtained χ^2 values do indicate good agreements with the data. This is because the correlations between the data points not shown in the figure have been considered [47].

The annihilation of halo DM also generates extra cosmic-ray antiparticles such as antiprotons and positrons. Compared with prompt gamma-rays, the prediction for cosmic-ray charged particles from DM annihilation suffers from large uncertainties in the cosmic-ray propagation models. For a DM particle mass ~ 60 GeV, the predicted \bar{p}/p ratio peaks at a lower energy ~ 10 GeV, which suffers from additional uncertainties due to the effect of solar modulation. The upper limits on the DM annihilation cross section from the AMS-02 and PAMELA data on \bar{p}/p ratio for various channels have been studied for a number of propagation models and DM density profiles (see e.g. [48–51]). In general, the obtained limits are weaker than that derived from the gamma rays of dSphs. Only in the extreme case with the “MAX” propagation model [52, 53] where the propagation parameters are adjusted to generate maximal antiproton flux while still be consistent with other comic-ray observables such as the

B/C flux ratio, the upper limits from \bar{p}/p can be compatible with that from the gamma rays for DM particle mass below ~ 100 GeV. The constraints from the cosmic-ray positrons are strongly dependent on the annihilation final states. For leptonic final states such as e^+e^- and $\mu^+\mu^-$, the derived upper limits from the AMS-02 positron flux can reach the typical thermal cross section for DM particle mass below 50–100 GeV [54]. But for hadronic final states such as $b\bar{b}$, the corresponding limits are rather weak, typically at $\mathcal{O}(10^{-24})$ cm³s⁻¹. The gg final state generates a softer positron spectrum in comparison with the $b\bar{b}$ final states. Thus the corresponding limits are expected to be even weaker.

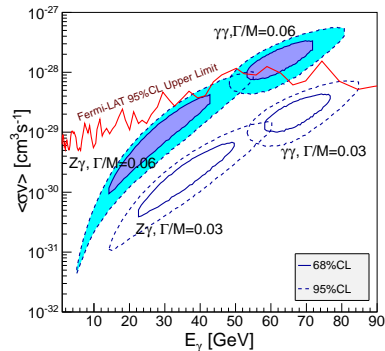


FIG. 2: Predictions for $\langle\sigma v\rangle_{\gamma\gamma}$ and $\langle\sigma v\rangle_{Z\gamma}$ as a function of photon energy using the allowed parameters from the fit to the data of diphoton exces and GCE with dijet limits included, for $\Gamma/M = 0.06$ and 0.03, respectively. The exclusion limits of Fermi-LAT [55] for region R16 are also shown.

Gamma-ray lines. Since ϕ couples to two photons, the DM particles inevitably annihilate into $\gamma\gamma$ ($Z\gamma$ if $g_1 \neq g_2$) with line-shape energy spectra at m_χ ($m_\chi(1 - m_Z^2/4m_\chi^2)$ for $Z\gamma$), which is difficult to be mimicked by conventional astrophysical contributions. The diphoton produced at LHC and from halo DM annihilation are strongly correlated. From Eq. (5) and (8) it follows that $\sigma_{\gamma\gamma}/\sigma_{jj} = \langle\sigma v\rangle_{\gamma\gamma}/\langle\sigma v\rangle_{gg}$. Therefore, a *lower* limit on $\langle\sigma v\rangle_{\gamma\gamma}$ can be derived from the upper limit on

the dijet production cross section

$$\langle\sigma v\rangle_{\gamma\gamma} \gtrsim 4.8 \times 10^{-30} \text{ cm}^3\text{s}^{-1} \left(\frac{\sigma_{\gamma\gamma}}{3.8 \text{ fb}} \right) \times \left(\frac{12 \text{ pb}}{\sigma_{jj}} \right) \left(\frac{r}{4.7} \right) \frac{\langle\sigma v\rangle_{gg}}{\langle\sigma v\rangle_0}, \quad (11)$$

where the reference value for $\sigma_{\gamma\gamma}$ is at its 2σ lower bound. The limit is roughly an order of magnitude lower than the current Fermi-LAT sensitivity. Making use of the determined parameters we obtain the predictions for $\langle\sigma v\rangle_{\gamma\gamma, Z\gamma}$ for $\Gamma/M = 0.06$ and 0.03 as shown in Fig. 2. The cross section for $Z\gamma$ channel is related to that of $\gamma\gamma$ as $\langle\sigma v\rangle_{Z\gamma} \approx \langle\sigma v\rangle_{\gamma\gamma}(1 - m_Z^2/4m_\chi^2)^3 g_{ZA}^2/2g_A^2$. For a comparison, the current 95% C.L. limits from the Fermi-LAT gamma line search based on Pass-8 data [55] for the ROI $16^\circ \times 16^\circ$ (R16) is also shown in Fig. 2. Since the Fermi-LAT limits are obtained assuming the Einasto profile, they are rescaled by a factor of 0.52 to compensate the differences in the J-factors, as we have adopted a contracted NFW profile. For $\Gamma/M = 0.06$ (0.03), the predicted typical cross section is $\mathcal{O}(10^{-28})$ ($\mathcal{O}(10^{-29})$) cm^3s^{-1} . As can be seen from Fig. 2, a significant portion of the parameter space is constrained by the current Fermi-LAT data for $\Gamma/M = 0.06$. But there is ample parameter space for lower values of Γ/M , such as for $\Gamma/M = 0.03$. Future experiments such as CALET and DAMPE are able to reach the lower limit of the cross section derived in Eq. (11) in the near future with larger statistics and higher energy resolutions.

In summary, we have shown that the reported photon excesses at LHC and GC can be simultaneously explained by a simple DM model. The best-fit DM particle mass is around 60 GeV and the annihilation cross section is typically thermal, which predicts that Γ/M of the resonance ϕ should be at least of $\mathcal{O}(10^{-2})$. The model predicts a minimal cross section of $\mathcal{O}(10^{-30}) \text{ cm}^3\text{s}^{-1}$ for DM annihilating into $\gamma\gamma$ which results in line-shape spectrum. Both of them are testable by the LHC, Fermi-LAT and future DM indirect detection experiments.

Acknowledgements. This work is supported by the NSFC under Grants No. 11335012 and No. 11475237.

-
- [1] LHC seminar, ATLAS and CMS physics results from Run 2, talks by Jim Olsen and Marumi Kado, CERN, 15 Dec. 2015. ATLAS note, ATLAS-CONF-2015-081, CMS note, CMS PAS EXO-15-004.
 - [2] R. Franceschini, G. F. Giudice, J. F. Kamenik, M. McCullough, A. Pomarol, R. Rattazzi, M. Redi, F. Riva, A. Strumia, and R. Torre (2015), 1512.04933.
 - [3] D. Buttazzo, A. Greljo, and D. Marzocca (2015), 1512.04929.
 - [4] CMS Collaboration, CMS-EXO-16-018.
 - [5] M. Low, A. Tesi, and L.-T. Wang (2015), 1512.05328.
 - [6] P. Agrawal, J. Fan, B. Heidenreich, M. Reece, and M. Strassler (2015), 1512.05775.
 - [7] Y. Mambrini, G. Arcadi, and A. Djouadi (2015), 1512.04913.
 - [8] M. Backovic, A. Mariotti, and D. Redigolo (2015), 1512.04917.
 - [9] X.-J. Bi, Q.-F. Xiang, P.-F. Yin, and Z.-H. Yu (2015), 1512.06787.
 - [10] D. Barducci, A. Goudelis, S. Kulkarni, and D. Sengupta (2015), 1512.06842.
 - [11] Y. Bai, J. Berger, and R. Lu (2015), 1512.05779.
 - [12] C. Han, H. M. Lee, M. Park, and V. Sanz (2015), 1512.06376.
 - [13] M. Bauer and M. Neubert (2015), 1512.06828.
 - [14] P. S. B. Dev and D. Teresi (2015), 1512.07243.
 - [15] H. Davoudiasl and C. Zhang (2015), 1512.07672.
 - [16] F. D'Eramo, J. de Vries, and P. Panci (2016), 1601.01571.
 - [17] L. Goodenough and D. Hooper (2009), 0910.2998.
 - [18] D. Hooper and L. Goodenough, Phys. Lett. **B697**, 412 (2011), 1010.2752.
 - [19] A. Boyarsky, D. Malyshev, and O. Ruchayskiy, Phys. Lett. **B705**, 165 (2011), 1012.5839.
 - [20] K. N. Abazajian, JCAP **1103**, 010 (2011), 1011.4275.
 - [21] D. Hooper and T. Linden, Phys. Rev. **D84**, 123005 (2011), 1110.0006.
 - [22] K. N. Abazajian and M. Kaplinghat, Phys. Rev. **D86**, 083511 (2012), [Erratum: Phys. Rev.D87,129902(2013)], 1207.6047.
 - [23] C. Gordon and O. Macias, Phys. Rev. **D88**, 083521 (2013), [Erratum: Phys. Rev.D89,no.4,049901(2014)], 1306.5725.
 - [24] O. Macias and C. Gordon, Phys. Rev. **D89**, 063515 (2014), 1312.6671.

- [25] K. N. Abazajian, N. Canac, S. Horiuchi, and M. Kaplinghat, *Phys. Rev.* **D90**, 023526 (2014), 1402.4090.
- [26] D. Hooper and T. R. Slatyer, *Phys. Dark Univ.* **2**, 118 (2013), 1302.6589.
- [27] W.-C. Huang, A. Urbano, and W. Xue (2013), 1307.6862.
- [28] T. Daylan, D. P. Finkbeiner, D. Hooper, T. Linden, S. K. N. Portillo, N. L. Rodd, and T. R. Slatyer (2014), 1402.6703.
- [29] F. Calore, I. Cholis, and C. Weniger, *JCAP* **1503**, 038 (2015), 1409.0042.
- [30] M. Ajello et al. (Fermi-LAT) (2015), 1511.02938.
- [31] R. Bartels, S. Krishnamurthy, and C. Weniger, *Phys. Rev. Lett.* **116**, 051102 (2016), 1506.05104.
- [32] S. K. Lee, M. Lisanti, B. R. Safdi, T. R. Slatyer, and W. Xue, *Phys. Rev. Lett.* **116**, 051103 (2016), 1506.05124.
- [33] D. Gaggero, M. Taoso, A. Urbano, M. Valli, and P. Ullio, *JCAP* **1512**, 056 (2015), 1507.06129.
- [34] L. Bian, N. Chen, D. Liu and J. Shu, arXiv:1512.05759; W. Liao and H. q. Zheng, arXiv:1512.06741; R. Ding, L. Huang, T. Li and B. Zhu, arXiv:1512.06560; M. x. Luo, K. Wang, T. Xu, L. Zhang and G. Zhu, arXiv:1512.06670; T. F. Feng, X. Q. Li, H. B. Zhang and S. M. Zhao, arXiv:1512.06696; F. Wang, L. Wu, J. M. Yang and M. Zhang, arXiv:1512.06715; X. F. Han and L. Wang, arXiv:1512.06587; W. C. Huang, Y. L. S. Tsai and T. C. Yuan, arXiv:1512.07268; J. Cao, C. Han, L. Shang, W. Su, J. M. Yang and Y. Zhang, arXiv:1512.06728; Q. H. Cao, Y. Liu, K. P. Xie, B. Yan and D. M. Zhang, arXiv:1512.05542; Q. H. Cao, Y. Liu, K. P. Xie, B. Yan and D. M. Zhang, arXiv:1512.08441.
- [35] R. D. Peccei and H. R. Quinn, *Phys. Rev. D* **16**, 1791 (1977); R. D. Peccei and H. R. Quinn, *Phys. Rev. Lett.* **38**, 1440 (1977); J. E. Kim, *Phys. Rept.* **150**, 1 (1987).
- [36] B. Gripaios, A. Pomarol, F. Riva, and J. Serra, *JHEP* **04**, 070 (2009), 0902.1483.
- [37] J. Ellis, S. A. R. Ellis, J. Quevillon, V. Sanz, and T. You, *JHEP* **03**, 176 (2016), 1512.05327.
- [38] J. Bernon and C. Smith, arXiv:1512.06113; W. S. Cho, D. Kim, K. Kong, S. H. Lim, K. T. Matchev, J. C. Park and M. Park, arXiv:1512.06824; S. Di Chiara, L. Marzola and M. Raidal, arXiv:1512.04939; F. P. Huang, C. S. Li, Z. L. Liu and Y. Wang, arXiv:1512.06732; J. Chang, K. Cheung and C. T. Lu, arXiv:1512.06671.
- [39] G. Aad et al. (ATLAS), *Phys. Rev.* **D91**, 052007 (2015), 1407.1376.
- [40] M. Ackermann et al. (Fermi-LAT), *Phys. Rev. Lett.* **115**, 231301 (2015), 1503.02641.
- [41] G. Aad et al. (ATLAS), *Eur. Phys. J.* **C76**, 45 (2016), 1507.05930.
- [42] G. Aad et al. (ATLAS), *Phys. Lett.* **B738**, 428 (2014), 1407.8150.
- [43] V. Khachatryan et al. (CMS), *JHEP* **10**, 144 (2015), 1504.00936.
- [44] G. Aad et al. (ATLAS), *JHEP* **01**, 032 (2016), 1509.00389.
- [45] T. Sjostrand, S. Mrenna, and P. Z. Skands, *Comput. Phys. Commun.* **178**, 852 (2008), 0710.3820.
- [46] P. Ullio and M. Valli (2016), 1603.07721.
- [47] F. Calore, I. Cholis, C. McCabe, and C. Weniger, *Phys. Rev.* **D91**, 063003 (2015), 1411.4647.
- [48] H.-B. Jin, Y.-L. Wu, and Y.-F. Zhou, *Phys. Rev.* **D92**, 055027 (2015), 1504.04604.
- [49] H.-B. Jin, Y.-L. Wu, and Y.-F. Zhou, *Int. J. Mod. Phys.* **A30**, 1545008 (2015), 1508.06844.
- [50] D. Hooper, T. Linden, and P. Mertsch, *JCAP* **1503**, 021 (2015), 1410.1527.
- [51] H.-B. Jin, S. Miao, and Y.-F. Zhou, *Phys. Rev.* **D87**, 016012 (2013), 1207.4408.
- [52] H.-B. Jin, Y.-L. Wu, and Y.-F. Zhou, *JCAP* **1509**, 049 (2015), 1410.0171.
- [53] H.-B. Jin, Y.-L. Wu, and Y.-F. Zhou, *JCAP* **1311**, 026 (2013), 1304.1997.
- [54] A. Ibarra, A. S. Lamperstorfer, and J. Silk, *Phys. Rev.* **D89**, 063539 (2014), 1309.2570.
- [55] M. Ackermann et al. (Fermi-LAT), *Phys. Rev.* **D91**, 122002 (2015), 1506.00013.